PHYSICAL REVIEW B **79**, 085102 (2009)

Order-*N* implementation of exact exchange in extended insulating systems

Xifan Wu, Annabella Selloni, and Roberto Car
Department of Chemistry, Princeton University, Princeton, New Jersey 08544-0001, USA
(Received 6 December 2008; revised manuscript received 11 January 2009; published 5 February 2009)

Exact (Hartree-Fock) exchange is needed to overcome some of the limitations of local and semilocal approximations of density-functional theory. So far, however, computational cost has limited the use of exact exchange in plane-wave calculations for extended systems. We show that this difficulty can be overcome by performing a unitary transformation from Bloch to maximally localized Wannier functions in combination with an efficient technique to compute real-space Coulomb integrals. The resulting scheme scales linearly with system size. We validate the scheme with representative applications.

DOI: 10.1103/PhysRevB.79.085102 PACS number(s): 71.15.Dx, 71.15.Mb, 71.15.Pd

I. INTRODUCTION

Electronic structure calculations based on density-functional theory (DFT) have been very successful in studies of molecular and condensed-matter systems. To date most DFT applications to extended material systems have used the local-density approximation (LDA) or the semilocal generalized gradient approximation (GGA) for exchange and correlation.[1] These approximations are numerically efficient but suffer from serious drawbacks. In particular, the spurious self-interaction of each electron with itself, occurring with local and semilocal functionals, may lead to a poor description of tightly bound electronic states.[2]

These deficiencies are less severe when hybrid functional approximations for exchange and correlation are adopted.[3,4] In this approach some exact exchange energy is mixed into the exchange-correlation energy functional. Extensive applications to molecular systems have shown that hybrid functionals are generally superior to GGA in the description of structural and electronic properties.[4] Applications to extended systems have been so far relatively scarce even though available studies suggest that hybrid functionals should provide a better description of the electronic properties of insulating materials.[5–7]

The main reason for the lack of applications of hybrid functionals to extended systems is the considerable computational cost of evaluating the exact exchange energy, particularly within the plane-wave-pseudopotential approach that is most frequently used for electronic structure calculations. This has limited most applications to systems with a small unit cell. When large supercells are needed, such as, e.g., in *ab initio* molecular-dynamics (AIMD) simulations,[8] a screened exchange approximation[9] is often used to alleviate the computational burden of hybrid functionals.[10]

In this work, we present an accurate and efficient scheme for computing the exact exchange energy and potential for large molecules and extended insulating systems. Our scheme can be easily included in existing plane-wave codes and has computational cost that scales linearly with system size. The approach is based on a unitary transformation of the occupied subspace from Bloch to (maximally) localized Wannier functions (MLWFs).[11] MLWFs are exponentially localized and, since the exchange between two orbitals is restricted to the spatial region of orbital overlap, the amplitude of the exchange interaction between two MLWFs decays rapidly with the distance between their centers. Thus, typically each Wannier orbital exchanges only with a finite number of neighboring orbitals and the number of pair interactions per orbital is independent of system size.[12] As a result, our procedure to compute exact exchange is order *N*, i.e., its computational cost scales linearly with system size. We demonstrate the effectiveness of our approach in two representative applications using the Perdew-Burke-Ernzerhof (PBE0) (Ref. 13) hybrid functional for exchange and correlation. In one we perform a ground-state electronic and structural optimization for crystalline silicon; in the other we perform a finite temperature AIMD simulation for the same system.

II. FORMALISM AND METHOD OF CALCULATION

In the following we assume, for simplicity, a closed-shell system with $N/2$ doubly occupied one-electron states. Extension to spin-polarized systems is straightforward. The PBE0 (Ref. 13) total-energy functional can be written as

$$E^{\mathrm{PBE0}} = -\frac{1}{2}\sum_i \langle \varphi_i|\nabla^2|\varphi_i\rangle + \int V_{\mathrm{ion}}(\mathbf{r})n(\mathbf{r})d\mathbf{r} + \frac{1}{2}\int\int \frac{n(\mathbf{r})n(\mathbf{r}')}{|\mathbf{r}-\mathbf{r}'|}d\mathbf{r}d\mathbf{r}' + E_{\mathrm{ion}}[\{\mathbf{R_I}\}] + E_{xc}^{\mathrm{PBE0}}, \tag{1}$$

where $n(\mathbf{r})=2\Sigma_{i=1}^{N/2}|\varphi_i(\mathbf{r})|^2$ is the electronic density, N is the total number of electrons, and the φ_i are the occupied one-electron orbitals, and atomic units (a.u.: $\hbar=m=e^2=1$) are adopted. As in standard DFT formulations using LDA or GGA functionals, the first four terms in Eq. (1) represent the electronic kinetic energy, the potential energy of the electrons in the field of the nuclei, the average electrostatic interaction among the electrons, and the electrostatic repulsion between the nuclei, respectively. Here we adopt a pseudopotential formulation. Thus the sums extend to the valence states only while $n(\mathbf{r})$ and φ_i denote pseudodensity and pseudowave functions, respectively. The last term on the right-hand side of Eq. (1) is the PBE0 exchange-correlation energy,[13] E_{xc}^{PBE0}, given by

$$E_{xc}^{\mathrm{PBE0}} = \frac{1}{4}E_x + \frac{3}{4}E_x^{\mathrm{PBE}} + E_c^{\mathrm{PBE}}. \quad (2)$$

Here E_x denotes exact exchange, E_x^{PBE} is the PBE exchange, and E_c^{PBE} is the PBE correlation functional.[14] The exact exchange energy E_x has the Hartree-Fock expression in terms of the one-electron (pseudo)orbitals:

$$E_x = -2\sum_{i,j}\int\int \frac{\varphi_i^*(\mathbf{r})\varphi_j^*(\mathbf{r}')\varphi_j(\mathbf{r})\varphi_i(\mathbf{r}')}{|\mathbf{r}-\mathbf{r}'|}d\mathbf{r}'d\mathbf{r}. \quad (3)$$

The ground-state energy is obtained by minimizing the energy functional [Eq. (1)] with respect to the occupied orbitals. This leads to the one-particle equations:

$$\left[-\frac{1}{2}\nabla^2 + V_{\mathrm{ion}}(\mathbf{r}) + V_H(\mathbf{r}) + \frac{3}{4}V_x^{\mathrm{PBE}}(\mathbf{r}) + V_c^{\mathrm{PBE}}(\mathbf{r})\right]\varphi_i(\mathbf{r}) + \frac{1}{4}\int V_x(\mathbf{r},\mathbf{r}')\varphi_i(\mathbf{r}')d\mathbf{r}' = \varepsilon_i\varphi_i(\mathbf{r}), \quad (4)$$

where $V_H(\mathbf{r})$ and $V_{\mathrm{ion}}(\mathbf{r})$ are the Hartree and the ionic (pseudo)potentials, respectively. $V_x^{\mathrm{PBE}}(\mathbf{r})$ and $V_c^{\mathrm{PBE}}(\mathbf{r})$, the PBE exchange and correlation potentials, depend on the electron density and its gradient at position $\mathbf{r}$. The exact exchange potential $V_x(\mathbf{r},\mathbf{r}')$ is the nonlocal integral operator of Hartree-Fock theory. It is given by

$$V_x(\mathbf{r},\mathbf{r}') = -2\sum_j \frac{\varphi_j^*(\mathbf{r}')\varphi_j(\mathbf{r})}{|\mathbf{r}-\mathbf{r}'|}. \quad (5)$$

We notice that the above procedure is not strictly a Kohn-Sham scheme. The latter would require an exchange potential given by the functional derivative of the exchange energy with respect to the electron density rather than with respect to the orbitals. Since the explicit functional dependence of the exact exchange energy on the density is not known, implementation of a strict Kohn-Sham scheme would require a special procedure such as, e.g., the optimized effective potential (OEP) method.[4] The latter would be considerably more computationally expensive than our approach while giving essentially the same ground-state energies.[4]

The action of $\hat{V}_x(\mathbf{r},\mathbf{r}')$ on the orbital φ_i in Eq. (4) is an orbital dependent term $D_x^i(\mathbf{r})$ given by

$$D_x^i(\mathbf{r}) \equiv \frac{\delta E_x}{\delta\varphi_i^*} = -2\sum_j \int d\mathbf{r}' \frac{\varphi_j^*(\mathbf{r}')\varphi_i(\mathbf{r}')\varphi_j(\mathbf{r})}{|\mathbf{r}-\mathbf{r}'|}. \quad (6)$$

Equation (6) shows that $D_x^i(\mathbf{r})$ includes the exchange interactions of the orbital φ_i with all the occupied orbitals φ_j (including the self-interaction). Usually in extended system implementations,[7] each pair interaction in Eq. (6) is evaluated in reciprocal space taking advantage of the convolution theorem[15]

$$\int d\mathbf{r}' \frac{\varphi_j^*(\mathbf{r}')\varphi_i(\mathbf{r}')}{|\mathbf{r}-\mathbf{r}'|} \rightarrow 4\pi\frac{\rho_{ij}(\mathbf{G})}{|\mathbf{G}|^2}, \quad (7)$$

where $\rho_{ij}(\mathbf{G})$ is the Fourier transform of $\rho_{ij}(\mathbf{r})=\varphi_i(\mathbf{r})\varphi_j(\mathbf{r})$. This can be calculated using the fast Fourier transform (FFT) algorithm at a cost proportional to $N_{\mathrm{FFT}}\ln(N_{\mathrm{FFT}})$, where N_{FFT} is the size of the plane-wave grid. Thus, if the functions $\{\varphi_i\}$ are delocalized throughout the entire supercell, evaluating Eq. (7) for all orbital pairs would result in an overall computational effort proportional to $N^2\times N_{\mathrm{FFT}}\ln(N_{\mathrm{FFT}})$. Neglecting the weak logarithmic dependence, this amounts to cubic scaling with size. While plane-wave LDA or GGA calculations have cubic scaling with size, they only require a number of FFTs that scales linearly with N. The need to perform a number of FFTs that scales quadratically with N is what makes traditional plane-wave implementations of the hybrid functional method very expensive.

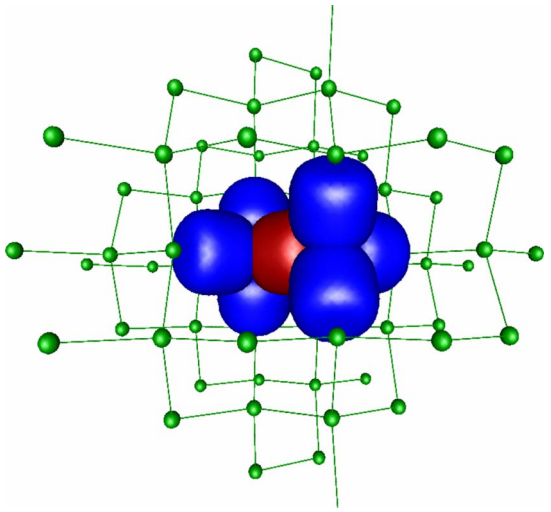

FIG. 1. (Color online) Overlap between a tagged Wannier orbital (red at the center) and its nearest neighboring Wannier orbitals (blue) in the 64-atom Si supercell. Si atoms are denoted by the green spheres.

Instead of evaluating the exact exchange in terms of delocalized Bloch orbitals $\{\varphi_i\}$, we choose to work with MLWFs $\{\tilde{\varphi}_i\}$. This requires a unitary transformation of the occupied subspace, $\tilde{\varphi}_i=\Sigma_{j=1}^{N/2}U_{ij}\varphi_j$, which leaves the ground-state energy invariant. In terms of the MLWFs $D_x^i(\mathbf{r})$ becomes

$$D_x^i(\mathbf{r}) = -2\left[v_{ii}(\mathbf{r})\tilde{\varphi}_i(\mathbf{r}) + \sum_{i\neq j} v_{ij}(\mathbf{r})\tilde{\varphi}_j(\mathbf{r})\right], \quad (8)$$

where the self-interaction (v_{ii}) and the pair-exchange (v_{ij}) potentials satisfy the Poisson equations

$$\nabla^2 v_{ii} = -4\pi\tilde{\rho}_{ii}, \quad \nabla^2 v_{ij} = -4\pi\tilde{\rho}_{ij}. \quad (9)$$

Here, $\tilde{\rho}_{ij}(\mathbf{r})=\tilde{\varphi}_i(\mathbf{r})\tilde{\varphi}_j^*(\mathbf{r})$. In the hybrid functional formalism the contribution associated to $v_{ii}(\mathbf{r})$ in Eq. (8) partially cancels the spurious self-interaction present in the Hartree potential $V_H(\mathbf{r})$ in Eq. (4). The contribution associated to the pair potential $v_{ij}(\mathbf{r})$ in Eq. (8) gives the exchange interaction for two electrons of equal spin residing in different orbitals. The potential v_{ij} (when i is either equal to or different from j) can be viewed as the electrostatic potential generated by the charge distribution $\tilde{\rho}_{ij}(\mathbf{r})$.

In the Wannier representation it is convenient to work in real space. This point is illustrated in Fig. 1. Since the exchange interaction is only present in the region where two

orbitals overlap, i.e., where $\tilde{\rho}_{ij} \neq 0$, the pair potential $v_{ij}(\mathbf{r})$ is conveniently calculated by solving the corresponding Eq. (9) in a spatial region significantly smaller than the simulation cell. Moreover only a small subset of orbitals $\tilde{\varphi}_j$ contributes to the exchange interaction with a tagged orbital $\tilde{\varphi}_i$.

We have implemented the above method in the CP code of the QUANTUM-ESPRESSO package.[16] In the following, we apply our approach to compute the electronic ground state, to optimize the cell parameter, and to carry out an AIMD simulation for crystalline Si in the diamond structure using the PBE0 functional. In these calculations we used supercells ranging from 64 to 216 atoms. In all the calculations we used a PBE norm-conserving pseudopotential with $(3s3p)$ valence. The plane-wave energy cutoff was 15 Ry and we sampled the Brillouin zone at the $k=0$ point (Γ point). For comparison we also performed PBE0 calculations with the same pseudopotential and plane-wave cutoff using the conventional reciprocal space method to calculate exact exchange as implemented in the PWSCF code of QUANTUM-ESPRESSO. These calculations were performed on the Si two-atom unit cell using a large set of k points to sample the Brillouin zone.

In our approach, we first perform a ground-state calculation using the semilocal PBE functional. Then, given the PBE Kohn-Sham eigenstates $\{\varphi_i(\mathbf{G})\}$, we construct the corresponding MLWFs $\{\tilde{\varphi}_i(\mathbf{G})\}$ (in reciprocal space) by iteratively minimizing the spread functional.[17] The corresponding MLWFs in real space, $\{\tilde{\varphi}_i(\mathbf{r})\}$, are obtained by FFT and are represented on a uniform real-space mesh. In the Si diamond structure, each MLWF is centered in the midpoint between two adjacent atoms and overlaps significantly with the six nearest neighboring orbitals, as shown in Fig. 1.

Since the density $\tilde{\rho}_{ij}(\mathbf{r})$ is known for each pair of orbitals, we can associate with each pair of orbitals an orthorhombic box with sides (l_x^c, l_y^c, l_z^c) such that, outside this box, $\tilde{\rho}_{ij}(\mathbf{r})$ is smaller than a given cutoff value ρ^{cut}, which we take as equal to 2×10^{-4} bohr^{-3} in the present work. We then solve Eq. (9) inside the box. Notice that the box contains a greatly reduced set of grid points compared to the simulation cell. For example, in our 64-atom Si calculation the real-space grid needed to compute the pair potential v_{ij} generated by two adjacent orbitals contains only 20% of the mesh points of the simulation cell. Even fewer points are needed to compute the pair potential $v_{ij}(\mathbf{r})$ generated by more distant orbitals. Since the density $\tilde{\rho}_{ij}(\mathbf{r})$ is vanishingly small when the distance between the orbitals i and j is sufficiently large, many pair interactions are negligibly small. We find that in our 64-atom Si supercell each orbital exchanges appreciably only with 30 orbitals out of the set of 127 neighboring orbitals.

To solve the Poisson equation the Laplace operator ∇^2 is discretized on seven mesh points. The resulting finite difference equation has the form of a linear matrix equation of the type $\mathbf{Ax}=\mathbf{b}$. The symmetric and positive-definite square matrix $\mathbf{A}$ is sparse and has dimension n, where n is the number of mesh points inside the reduced box. The vector $\mathbf{x}$ corresponds to the unknown $v_{ij}(\mathbf{r})$, and the (known) vector b corresponds to the pair density $\tilde{\rho}_{ij}(\mathbf{r})$. The values of $v_{ij}(\mathbf{r})$ at the boundary of the box are set by the multipole expansion

$$v_{ij}(\mathbf{r}) = 4\pi \sum_{l,m} \frac{1}{2l+1} q_{lm} \frac{Y_{lm}(\theta,\phi)}{r^{l+1}}, \tag{10}$$

where the multipoles q_{lm} are given by the integrals

$$q_{lm} = \int Y_{lm}^*(\theta',\phi') r'^l \tilde{\rho}_{ij}(\mathbf{r}') d\mathbf{r}'. \tag{11}$$

In Eq. (11) the Y_{lm} are spherical harmonics referred to the center of the pair density, which we define by $\mathbf{R}_{ij}^c \equiv \int \mathbf{r}\tilde{\rho}_{ij}(\mathbf{r}) / \int \tilde{\rho}_{ij}(\mathbf{r})$. We found that inclusion of multipoles up to $l=6$ is sufficient to achieve good accuracy.

Solving the linearized Poisson equation $\mathbf{Ax}=\mathbf{b}$ is equivalent to finding the vector $\mathbf{x}$ that minimizes the function $f(\mathbf{x}) = \frac{1}{2}\mathbf{x}^T\mathbf{Ax} - \mathbf{b}^T\mathbf{x} + c$, where c is an arbitrary constant. This minimization is efficiently performed with the conjugate gradient (CG) method.[18] We terminate the CG iteration when the residue in the calculation of $v_{ij}(\mathbf{r})$ is everywhere smaller than 10^{-5} a.u. In order to calculate the D_x^i in Eq. (8) we need to evaluate the products $v_{ij}(\mathbf{r})\tilde{\varphi}_j(\mathbf{r})$ in the region where $|\tilde{\varphi}_j(\mathbf{r})|^2 > \rho^{\text{cut}}$. This region may include points outside the box associated to the pair density $\tilde{\rho}_{ij}(\mathbf{r})$ but values of $v_{ij}(\mathbf{r})$ outside that box are easily obtained from the multipole expansion in Eq. (10).

Having calculated the $D_x^i(\mathbf{r})$, the PBE0 ground state is obtained by conventional electronic structure methods. Here we optimize the electronic degrees of freedom via damped second-order Car-Parrinello dynamics[8,19] in which the "force" acting on the orbitals, $H^{\text{PBE0}}\tilde{\varphi}_i(\mathbf{r})$, includes the additional $D_x^i(\mathbf{r})$ terms to account for exact exchange. Finally, the exchange energy E_x is given by the sum of the energies of the orbital pairs in the presence of the corresponding pair potential $v_{ij}(\mathbf{r})$,

$$E_x = -2\sum_{ij} \int \tilde{\varphi}_i(\mathbf{r})\tilde{\varphi}_j(\mathbf{r}) v_{ij}(\mathbf{r}) d\mathbf{r}. \tag{12}$$

The exchange energy in Eq. (12) can be viewed as a sum of orbital contributions $e_x(i): E_x = \Sigma_i e_x(i)$. The ith orbital contribution $e_x(i)$ can be further decomposed into self-exchange $e^{\text{self}}(i) = \int \tilde{\varphi}_i^2 v_{ii}$ and pair-exchange $e^{\text{pair}}(i) = \Sigma_{j\neq i} \int \tilde{\varphi}_i \tilde{\varphi}_j v_{ij}$.

TABLE I. Contributions to the exchange energy e_x (in a.u.) from shells of neighbors. $R(I)$ is shell radius (bohr) and $N(I)$ is the coordination number of shell I. The experimental lattice constant $a_0 = 5.43$ Å is used.

Shell I	0	1	2	3	4
$R(I)$	0	3.63	6.28	7.26	8.11
$N(I)$	1	6	12	12	12
$e_x(I)$	−0.465	−0.059	−0.002	−0.007	−0.0001

TABLE II. Comparison of our real-space method and the reciprocal space method implemented in PWSCF. E denotes total (pseudo) energy per atom (Rd) and VBW is the valence bandwidth (eV).

	Our approach		PWSCF	
k points	Gamma		$4\times4\times4$	$6\times6\times6$
N_{atom}/cell	64	216	2	2
E	−7.865	−7.870	−7.867	7.873
VBW	13.3	13.3	13.3	13.3

III. RESULTS AND DISCUSSION

In Table I we report the calculated exchange energy per orbital in crystalline Si using a 64-atom supercell. In this system the MLWFs are all equivalent by symmetry, i.e., the orbital index in $e_x(i)$ can be dropped. Moreover the MLWF centers coincide with the bond centers and it is convenient to group the pair-exchange contributions into contributions originating from the different shells of neighbors of a bond center. The table lists the shell index I (which is zero for the central site, one for the first shell of neighbors, etc.), the corresponding shell radius $R(I)$, the corresponding coordination number $N(I)$, and the corresponding exchange energy contribution $e_x(I)$, with $e_x=\Sigma_I e_x(I)$.

It is evident that the largest contribution to e_x comes from the self-interaction $e_x(0)$, and that the exchange contributions of the neighboring shells, $e_x(I)$, with $I=1,2,\ldots$, goes rapidly to zero with increasing shell radius. As a matter of fact the exchange energy contribution of the fourth shell is only 1/300th of the contribution due the first shell of neighbors.

In Table II, we report the calculated PBE0 ground-state energy using two supercells: one with 64 atoms and one with 216 atoms. The results of the two calculations are compared to the results obtained with the conventional reciprocal space method using a two-atom unit cell. In the case of the two large supercells we used Γ point sampling while we used two large sets of k points in the conventional calculations as indicated in the table. The two sets of calculations are in very close agreement: the valence bandwidths (VBWs) are the same while the slight differences in total energy can be attributed to the differences in the k-point sampling.

As a further comparison we report in Table III the equilibrium lattice constant a_0 and the bulk modulus B_0 calculated with a 64-atom Si supercell. We also report in the same table the results of a conventional calculation with a two-atom unit cell and a $4\times4\times4$ k-point grid. Again, the results of the two calculations are in excellent agreement.

In our approach, the computational cost of an exact exchange calculation depends on the number of pair exchanges that need to be included to achieve a desired accuracy. Since each orbital has exchange only with a finite number of neighboring orbitals independently of the system size, the computational effort of the exact exchange calculation should scale linearly with system size. Figure 2 shows that this is indeed the case.

TABLE III. Lattice constant a_0 (Å) and bulk modulus B_0 (GPa) of a Si.

	Our approach	PWSCF	Expt.[a]
a_0	5.49	5.49	5.43
B_0	100	99	99

[a]Reference 20.

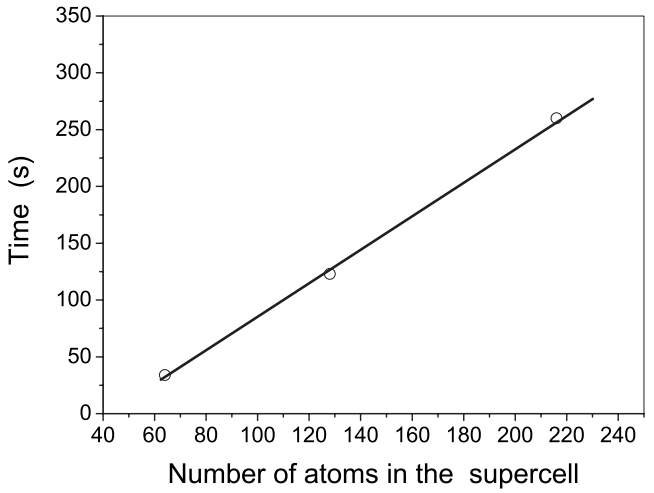

FIG. 2. Computational cost of exact exchange per iteration of AIMD dynamics with different supercells. The computational cost is given by the time (s) necessary to compute exact exchange on a 16-CPU 3.2 GHz Intel Xeon computer cluster.

Finally, we demonstrate that our approach makes AIMD simulations with hybrid functionals, such as PBE0, feasible at a modest computational cost. In AIMD simulations a large number of time steps, typically tens of thousands, are necessary to obtain statistically meaningful results. As a consequence AIMD simulations with hybrid functionals are very challenging and so far have only been performed by making some approximation, such as the screened exchange approximation, in the calculation of the exchange integrals.[10] In our approach we do not need to modify the Coulomb potential to eliminate exchange interactions at large distance. These are automatically truncated by the exponential decay of the MLWFs and all the relevant pair-exchange interactions are included. To show the feasibility of AIMD simulations, we tested our approach in a finite temperature simulation of a Si sample with 64 atoms in a simple-cubic supercell geometry. The simulation was initiated by randomly displacing the atoms from their crystalline sites while their velocities were set to zero. The subsequent trajectories were obtained by numerically integrating the Car-Parrinello equations of motion with the standard Verlet algorithm.[21] MLWF-based AIMD trajectories were generated as described in Ref. 17, using the PBE0 total-energy functional E^{PBE0} to compute the forces on electronic and ionic degrees of freedom.

We plot in Fig. 3 the time variation along a nuclear trajectory of E^{PBE0}, i.e., the potential energy of the ions (nuclei plus core electrons), of their kinetic energy $K=1/2\Sigma_I M_I \dot{R}_I^2$, and of the ionic internal energy $U=K+E^{PBE0}$. The internal energy is an exact constant of motion of classical nuclear dynamics but is only approximately constant in Car-Parrinello simulations due to the fictitious dynamics of the electrons. Figure 3 shows that indeed U is approximately

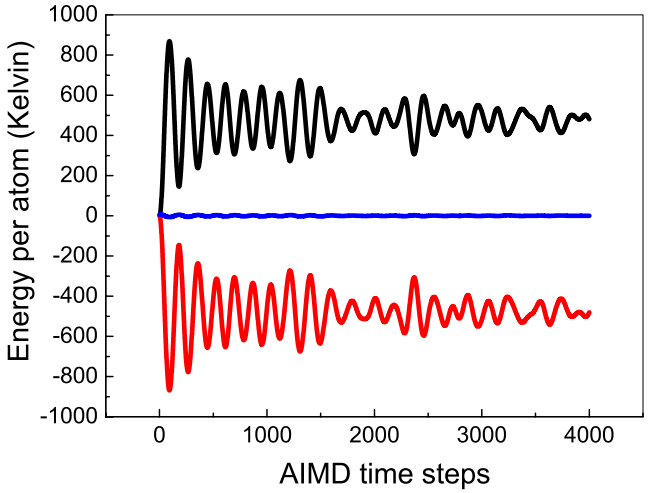

FIG. 3. (Color online) Potential energy per atom E^{PBE0} (red line), kinetic energy per atom K (black line), and internal energy per atom U (blue line) vs AIMD time steps. The average U sets the zero of the energy scale. A time step $\Delta=8$ a.u. and a fictitious electronic mass of 800 a.u. were used.

constant with minor fluctuations and no drift over the time scale of the simulation. This is the typical behavior observed in standard simulations of insulating systems based on LDA or GGA functionals. We conclude that our real-space treatment of exact exchange does not lead to any appreciable degradation of the quality of the integrated trajectories compared to standard AIMD simulations.

The AIMD trajectory reported in Fig. 3 was obtained on a 16 CPU PC cluster and took 34 s of real time per time step. For comparison a standard GGA simulation for the same system would take only 2.5 s per time step on the same computational platform. This example shows that while hybrid functional calculations remain more expensive than GGA calculations, AIMD trajectories lasting for many ps are possible with access to moderate computer resources. Moreover the order-N cost of the exact exchange calculation means that the overhead of hybrid functional calculations should be a comparatively smaller fraction of the overall computational cost in simulations on bigger systems.

IV. SUMMARY

In conclusion we have developed an order-N method to compute exact exchange in extended insulating systems. By exploring the locality of maximally localized Wannier functions, we calculate the orbital dependent exchange potential and the corresponding exchange energy contribution directly in real space. The approach is sufficiently efficient to make AIMD simulations with hybrid functionals possible and can be effectively implemented on parallel computer platforms. Its computational efficiency should be even better for large band-gap systems such as, e.g., water, where the MLWFs are more localized than in silicon. Since exact exchange is a basic ingredient in many-body approaches to electronic excitations, such as, e.g., the GW scheme,[22] our approach should facilitate the application of these schemes to systems requiring large supercells, such as liquids and disordered systems in general.[23]

ACKNOWLEDGMENTS

We would like to thank Morrel H. Cohen, Eric Walter, and Andrew Rappe for useful discussions. This work has been supported by the Department of Energy under Grants No. DE-FG02-06ER-46344 and No. DE-FG02-05ER46201, and by AFOSR-MURI Contract No. F49620-03-1-0330.

[1] See, e.g., R. G. Parr and W. Yang, *Density Functional Theory of Atoms and Molecules* (Oxford University Press, New York, 1989).
[2] A. J. Cohen, P. Mori-Sanchez, and W. Yang, Science **321**, 792 (2008).
[3] A. D. Becke, J. Chem. Phys. **98**, 1372 (1993).
[4] S. Kümmel and L. Kronik, Rev. Mod. Phys. **80**, 3 (2008).
[5] F. Corà, M. Alfredsson, G. Mallia, D. S. Middlemiss, W. C. Mackrodt, R. Dovesi, and R. Orlando, Struct. Bonding (Berlin) **113**, 171 (2004).
[6] J. F. Dobson, M. J. Bünner, and E. K. U. Gross, Phys. Rev. Lett. **79**, 1905 (1997).
[7] M. Marsman, J. Paier, A. Stroppa, and G. Kresse, J. Phys.: Condens. Matter **20**, 064201 (2008).
[8] R. Car and M. Parrinello, Phys. Rev. Lett. **55**, 2471 (1985).
[9] J. Heyd and G. E. Scuseria, J. Chem. Phys. **118**, 8207 (2003).
[10] T. Todorova, A. Seitsonen, J. Hutter, I-Feng Kuo, and C. Mundy, J. Phys. Chem. B **110**, 3685 (2006).
[11] N. Marzari and D. Vanderbilt, Phys. Rev. B **56**, 12847 (1997).
[12] N. Marzari, I. Souza, and D. Vanderbilt, Psi-K Newsletter **57**, 129 (2003).
[13] J. P. Perdew, M. Ernzerhof, and K. Burke, J. Chem. Phys. **105**, 9982 (1996).
[14] J. P. Perdew, K. Burke, and M. Ernzerhof, Phys. Rev. Lett. **77**, 3865 (1996).
[15] We assume here that the periodic supercell is sufficiently large that the sampling of the Brillouin zone can be limited to the $k=0$ point only.
[16] See http://www.quantum-espresso.org and http://www.pwscf.org
[17] M. Sharma, Y. Wu, and C. Car, Int. J. Quantum Chem. **95**, 821 (2003).
[18] W. H. Press, S. A. Teukolsky, W. T. Vetterling, and B. P. Flannery, *Numerical Recipes* (Cambridge University Press, Cambridge, 1992).
[19] F. Tassone, F. Mauri, and R. Car, Phys. Rev. B **50**, 10561 (1994).
[20] J. Heyd and G. E. Scuseria, J. Chem. Phys. **121**, 1187 (2004).
[21] R. Car, in *Conceptual Foundations of Materials: A Standard Model for Ground- and Excited-State Properties, Contemporary Concepts of Condensed Matter Science*, edited by S. G. Louie and M. L. Cohen (Elsevier, Amsterdam, 2006), Chap. 3, p. 64.
[22] L. Hedin, Phys. Rev. **139**, A796 (1965).
[23] W. Chen, X. Wu, and R. Car (unpublished).